ADVANCED FUNCTIONAL MATERIALS
www.afm-journal.de

Nanowire Based Mechanostimulating Platform for Tunable Activation of Natural Killer Cells

*Viraj Bhingardive, Avishay Edri, Anna Kossover, Guillaume Le Saux, Bishnu Khand, Olga Radinsky, Muhammed Iraqi, Angel Porgador, and Mark Schvartzman**

The understanding of the activation mechanism of natural killer (NK) cells has been traditionally based on the biochemical interaction of NK cell receptors with the ligands presenting on target cells. Yet, how physical features of the NK cell environment, such as stiffness and nanoscale topography, regulate the activity of NK cells, is unknown. An artificial microenvironment is developed for NK cell stimulation based on variably elongated nanowires functionalized with activating antigens and used it as a tunable model system to study the separate and cumulative effects of elasticity and nanotopography on NK cell activation. It is found that late signaling, degranulation, and cytokine production in NK cells consistently vary with nanowire length, and it is maximized for the longest nanowires, measuring ≈20 µm in length. Intriguingly, a similar trend is observed for nanowires lacking antigens, albeit with a lower activation magnitude overall, indicating that chemical and mechanical stimuli independently determine the activation of NK cells. The demonstrated tuning of the activation of NK cells by nanoscale physical features of their environment not only provides an important insight into the regulation mechanism of these lymphocytes, but also paves the way to rationally designed nanomaterials for controlled ex vivo activation of NK cells in immunotherapy.

1. Introduction

Natural Killer (NK) cells – cytotoxic lymphocytes that play a central role in our innate immune system – provides the first line of defense against viral and bacterial invasions, as well as against tumor development, by directly attacking cells expressing stress induced ligands.[1–3] It is well established that the cytotoxic activity of NK cells is regulated by a subtle balance between multiple activating, costimulatory, and inhibitory receptors that recognize specific ligands expressed by somatic cells.[4–6] On the other hand, very little is known about how the cytotoxic activity of NK cells is regulated by the physical features of their environment, such as mechanical elasticity and topography. In contrast to T cells and B cells, whose mechanical sensing has been extensively studied in the last decade,[7–10] the first evidence for the mechanical sensing of NK cells came only lately. Matalon et al. recently demonstrated that actomyosin retrograde flow regulates the immune response of NK cells, thereby demonstrating the mechanotransducive conversion of actomyosin forces into activating signals.[11] Also, direct evidence for the mechanosensing of NK cells was recently provided by our group, by demonstrating that primary NK cells produce boosted degranulation while stimulated ex vivo on a dense forest of nanowires functionalized with activating ligands.[12] This boosted degranulation was associated with the ultra-high compliance of the nanowires to centripetal mechanical forces applied by NK cells, and provide a support for a long-standing hypothesis that NK cells, similarly to T cells, apply mechanical forces to probe their target cells, and decide whether the latter should be attacked or tolerated. Another mechanostimulating effect could potentially stem from the topography of the nanowires, which shaped the morphology of the stimulated NK cells by forming long invaginations within the cell membrane. Such a topography mimics the morphology of professional antigen presenting cells such as dendritic cells, which interact in vivo with NK cells with long protrusions (dendrites) that elongate during the dendritic cell maturation.[13] Dendritic cells also express **MHC class I** polypeptide–related sequence A (MICA) that provide a chemical stimulus for the activation of NK cells.[14–17] Although the exact role of both morphology and mechanical stiffness of dendritic cells in their function is still largely unclear, recent studies have showed that dendritic cells increase their elasticity during their development, which in turn modifies their ability to activate T cells.[18]

Understanding the cell response mechanism to physical stimuli is extremely challenging by using standard biological

Dr. V. Bhingardive, A. Kossover, Dr. G. L. Saux, Prof. M. Schvartzman
Department of Materials Engineering
Ben-Gurion University of the Negev
P.O. Box 653, Beer-Sheva 84105, Israel
E-mail: marksc@bgu.ac.il

Dr. V. Bhingardive, A. Kossover, Dr. G. L. Saux, Prof. M. Schvartzman
Ilse Katz Institute for Nanoscale Science and Technology
Ben-Gurion University of the Negev
P.O. Box 653, Beer-Sheva 84105, Israel

Dr. A. Edri, Dr. B. Khand, Dr. O. Radinsky, M. Iraqi, Prof. A. Porgador
The Shraga Segal Department of Microbiology
Immunology, and Genetics Faculty of Health Sciences
Ben-Gurion University of the Negev
P.O. Box 653, Beer-Sheva 84105, Israel

The ORCID identification number(s) for the author(s) of this article can be found under https://doi.org/10.1002/adfm.202103063.

DOI: 10.1002/adfm.202103063

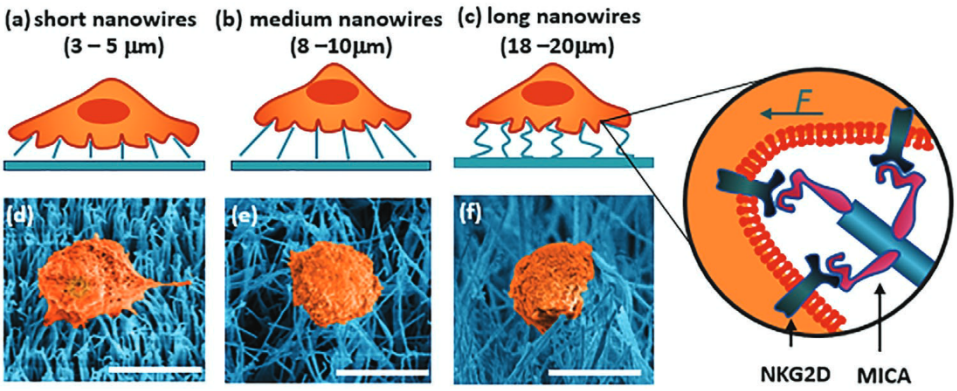

Figure 1. a,b) Schematic illustration of the activation of NK cell on ligand functionalized nanowires. d,e) False colored SEM images of NK cells stimulated on short, medium, and long nanowires. Scale bar – 10 µm.

methods, for several reasons. First, the natural cell environment is highly diverse, complex, and multifaceted, and it delivers numerous physical stimuli simultaneously. These stimuli intermix and produce a cumulative cell response, in which the role of each stimulus cannot be determined. Second, many of these stimuli physically span nanometric scales, and resolving them is challenging even when using advanced super-resolution microscopies. Finally, the physical stimuli in the natural cell environment cannot be deterministically controlled, thus the effect of the magnitude of each stimulus on cell response cannot be systematically studied. All these limitations can be overcome by a "reductionist" approach, in which cells are stimulated in a surrogate microenvironment that artificially produces specific stimuli in a controllable and deterministic manner. Then, studying the cell response to the variation in the artificial stimulus enables a systematic study of its mechanism.

Engineering reductionist microenvironments for controlled cell stimulations has emerged nowadays thanks to recent advances in nanomaterials and nanotechnology. Many of these advances have been applied to study how physical environmental factors that span over the nanometric scale regulate vital cell functions, including but not limited to cell adhesion,[19–21] mechanotransduction,[22] and differentiation.[23] In the context of the immune function, the role of the physical arrangement of extracellular ligands in the activation of T cells and NK cells has been studied using nanofabricated stimulating platforms, in which individual ligands were precisely positioned by block-copolymer[24–26] electron-beam,[27] and nanoimprint[28] lithography. Nanofabricated ligand patterns were also used to elucidate the effect of the ligand arrangement on the morphology of T cells.[29] The role of the size-based spatial exclusion of T cell receptors from large signaling molecules has been recently examined using 3D nanostructured patterns, in which the ligands were controllably positioned perpendicularly to the plane of the cell membrane.[27] Similarly, nanostructured patterns for T cell simulation were used to study the effect of the receptor dimensions in their organization within the cell membrane.[30] These and many other examples illustrate an intriguing approach of applying nanomaterials and nanostructures in fundamental biological studies, yet, at the same time, they emphasize the apparent challenges of this approach. First, each such nanomaterial or nanostructure should be rationally designed and fine-tuned to address a specific biological question. Second, such nanomaterials or nanostructures must be often integrated with biochemical functionalities, which are relevant for the natural cell environment, and are essential for providing necessary biochemical stimuli complementary to the physical ones.

Here, we developed a nanowire-based platform for the tunable mechano- stimulation of NK cells, and used it to elucidate the separate effects of the elasticity and nanotopography of the NK cell environment on their immune function. The platform was based on a dense forest of nanowires, whose length varied. For the study described here, we produced nanowires with lengths of three discrete ranges: 3–5, 8–10, and 18–20 µm, which are termed hereafter as short, medium, and long nanowires. It should be noted that, regardless of length, the portion of the nanowires with which NK cells interact corresponds to the ≈2 µm at their distal ends, and thus produce the same topographic environment for NK cells. For this same reason, all nanowires types produce the same amount of chemical stimulus, which is provided by activating ligands immobilized on the surface (**Figure 1**a). On the other hand, differently elongated nanowires had strikingly different bending moduli, and thus produced systematically varied mechanical stimuli for the activation of NK cells. We found that the nanowires stimulated cell contraction and induced a nearly similar cell morphology that included invaginations of the nanowires into the cell membrane, with no dependence on nanowire length. Oppositely, nanowire length greatly affected the signaling and the immune response of NK cells, as characterized by variations in the degree of nuclear translocation of NF-κB, the secretion of Interferon gamma (IFN- γ), and the expression of the degranulation marker CD107a – which all significantly increased with nanowire length. These findings demonstrate NK cells sense the elasticity of the stimulating environment, and that this elasticity is an important stimulus whose magnitude can promote or impede the immune response of NK cells.

2. Results

ZnO nanowires with an average diameter of 50 nm (Figure S1d, Supporting Information) were grown on A-plane sapphire

substrate in a custom-made chemical vapor deposition (CVD) system using the vapor-liquid-solid (VLS) approach,[31–33] and functionalized with **MICA**,[12] which is an activating ligand for NK cells. (Details appear in Figure S2 in the Supporting Information). By controlling the nanowire growth time, we produced dense forests of differently elongated nanowires, which provided the same topographic microenvironment for the stimulation of NK cells, yet strikingly different microenvironments in terms of their mechanical response to the forces applied by NK cells. Indeed, the bending modulus of an individual vertical nanowire, which is defined as the ratio between the horizontal force applied on the nanowire tip and its horizontal deflection, can be calculated from the formula of the bending of a cantilever with a circular cross-section[34]

$$f/\delta = 3\pi E r^4/4l^3 \quad (1)$$

Here, f is horizontal force, δ is horizontal deflection, l is the nanowire length, E the Young modulus of the nanowire material, and r is the nanowire radius. Thus, a dense forest of nanowire would produce a cumulative shear modulus τ that can be defined as the ratio between the applied horizontal stress (i.e., force per area) and the horizontal bending normalized to the nanowire length

$$\tau = \frac{F/A}{\delta/l} = \frac{N}{A}\frac{fl}{\delta} = \frac{N}{A}\frac{3\pi E r^4}{4l^2} \quad (2)$$

Taken that the average literature value of Young modulus of ZnO is 45 GPa,[35–38] this results in shear moduli of about 2.5 kPa, 500 Pa, and 100 Pa for the forest of short, medium, and long nanowires, respectively. This stiffness range is physiologically relevant, since it corresponds to the range within which dendritic cells modulate their stiffness upon inflammation[39] or maturation.[18] As such a low elasticity can be hardly implemented for elastomers that have been commonly used for the study of mechanosensing,[8,9,40,41] our nanowire-based mechanostimulatory platform provides an ideal artificial microenvironment for the systematic study of the mechanosensing of NK cells.

At first, we studied how the nanowire length affects the morphology of NK cells. To that end, we incubated NK cells on the nanowires for 3 hours, fixed them, and imaged them by confocal microscope in z-stack mode. To separate between the mechano-stimulatory effect provided by the nanowires, and the chemo-stimulatory effects provided by the immobilized MICA ligands, we also used three types of control surfaces: (i) sapphire surface with nanowires of all the tested lengths but without MICA functionalization, which produced the mechanical stimulus only, (ii) sapphire substrate covered with Au nanoparticles functionalized with MICA similarly to the nanowires, which produced the chemical stimulus only, and (iii) sapphire surface covered with Au nanoparticles without MICA functionalization, which lacked both stimuli. We first verified that the nanowires invaginated the cell membrane, by staining the membrane with a CellMask label (white). By this way, we could detect the projection in the membrane formed along the nanowire invaginations, and also verify that the nanowires are bent upon the centripetal forces applied by

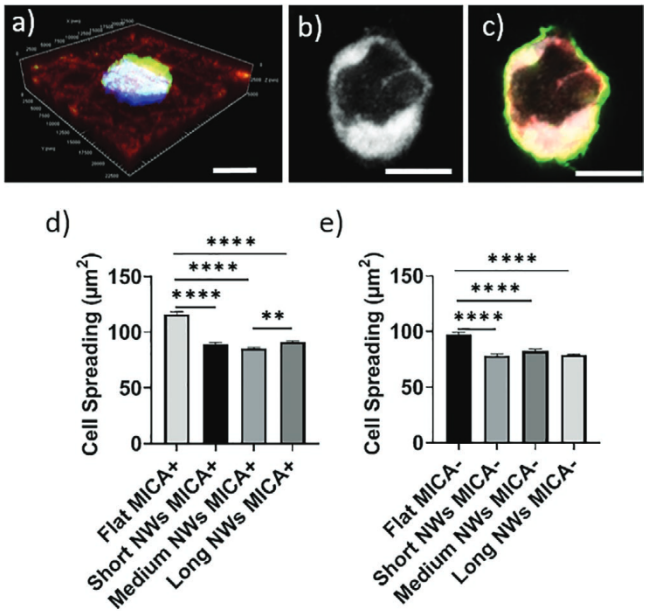

Figure 2. a) Confocal 3D image of NK cell stimulated on MICA-functionalized nanowires. Cytoskeleton (green), nucleus (blue), cell membrane (white) and nanowires (red) (Scale bar 10 μm). b,c) Z-stack confocal image of NK cell with fluorescently tagged membrane onto MICA-functionalized nanowires. The cell membrane is shown in b) white, and c) nanowires and actin are in red and green respectively (Scale bar 5 μm). d) Cell-spreading onto MICA-functionalized flat surfaces and surfaces with nanowires. e) Cell-spreading onto non-functionalized flat and nanowire surfaces. Cell spreading was quantified by measuring the projected area of the cells. The analysis was performed with Tukey's multiple-comparison tests using the GraphPad Prism software. *$p < 0.05$, **$p < 0.01$, ***$p < 0.001$, ****$p < 0.0001$, ns-not significant. (+) and (–) mean surfaces with and without MICA functionalization, respectively.

the cells. We then quantified the projected areas of the cells (Figure 2d). We found that NK cells stimulated on a flat MICA-functionalized surface showed an average projected area of about 120 μm^2. This area is significantly higher compared to that of cells stimulated on the nanowires. Interestingly, neither the nanowire length nor the functionalization significantly affected the cell area. It can be concluded therefore that NK cells contract on a mechanically compliant surface down to a certain area, and that the mechanical compliance of the nanowires of all the three probed lengths was high enough to allow this contraction. On the other hand, this contraction is independent of the presence of the activating chemical stimulus, as the cells stimulated on bare nanowires indicate. The effect of chemical stimulus is, however, different for flat rigid surfaces: flat MICA-functionalized surfaces yielded a much higher cell spreading than bare flat surfaces. This result stems from the fact that the morphology of NK cells is regulated, in particular, by the interaction of their activating receptors NKG2D with MICA. Still, the effect of MICA vanishes when it is grafted onto nanowires, whose flexibility and compliance to the forces applied by NK cells supersedes the influence of MICA-NKG2D interaction on cell morphology.[42]

Whereas the morphology of NK cells stimulated on the nanowires can provide information on how these cells interact with a nanotopographic and elastic environment, it alone

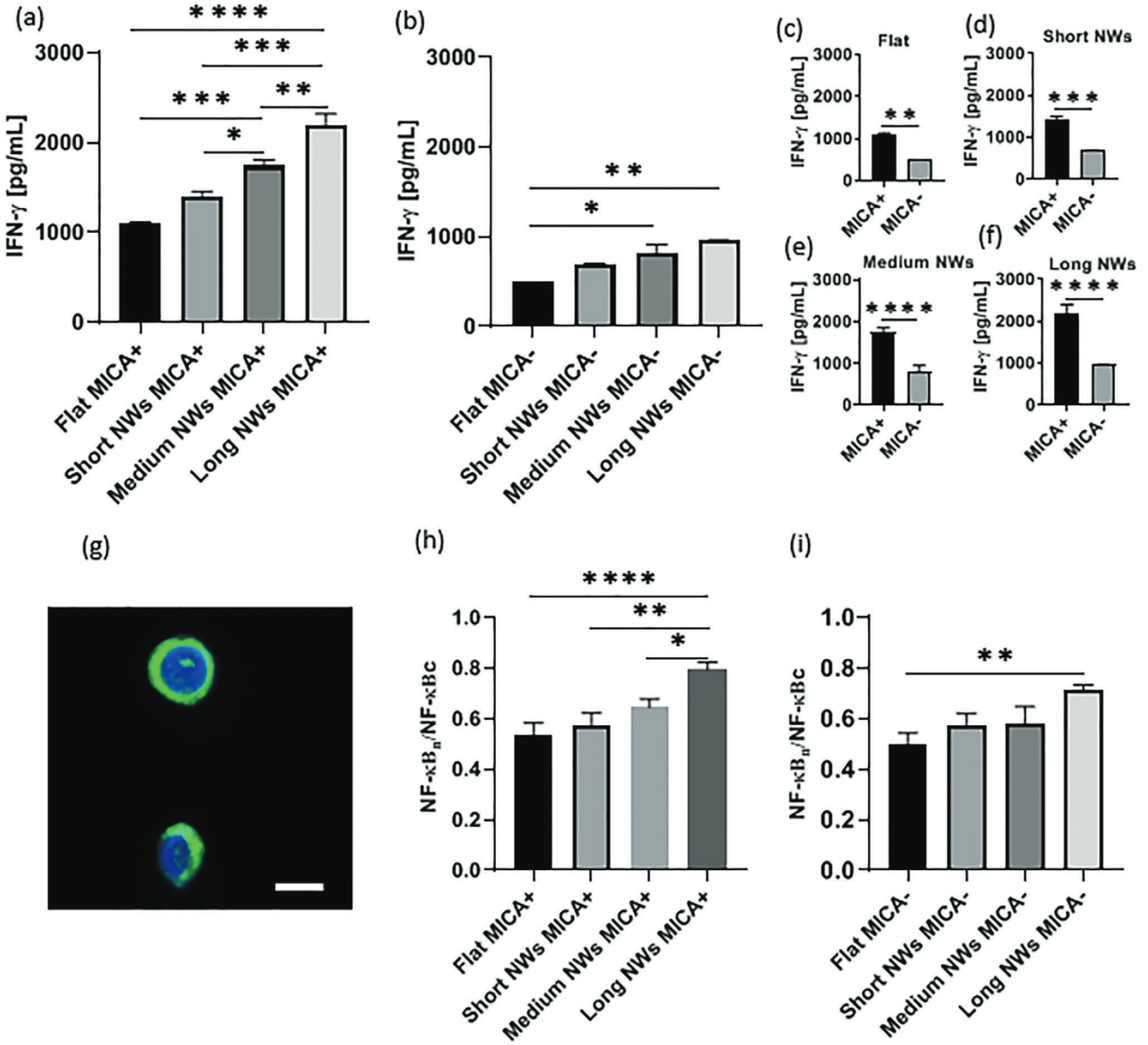

Figure 3. a,b) Quantification of IFN-γ secretion by NK cells activated on flat surfaces and surfaces with nanowires with and without MICA, respectively. c-f) Effect of MICA-functionalization on the activation of NK cells on flat, short, medium, and long nanowire surfaces, respectively. g) NF-κB p65 staining (green) of activated NK cells (Scale bar 5 µm). h,i) The degree of nuclear NF-κB translocation was determined by confocal imaging and expressed as the ratio of nuclear to cytoplasmic p65 subunit from surfaces with and without functionalization. The analysis was performed with Tukeys' multiple-comparison tests using the GraphPad Prism software. *$p < 0.05$, **$p < 0.01$, ***$p < 0.001$, ****$p < 0.0001$, ns-not significant. (+) and (–) mean surfaces with and without MICA functionalization, respectively.

is not an indicator for the functional response of NK cells to the environmental topography and elasticity. To evaluate this response, we quantified the secretion of interferon-γ, which is the primary marker for the cytotoxic activity of NK cells. To that end, NK cells were incubated on the tested surfaces for 24 hours, and the supernatant was analyzed by a standard ELISA protocol (See the Supporting Information). To ensure that the cells are exposed to the same conditions, all the surfaces, including control surfaces, were mounted on specially designed holders that exposed a constant surface area for cell seeding, and made use of a constant volume of cell medium.

Results of interferon-γ measurements are shown in Figure 3a–f. First, Figure 3a indicates that, in the presence of MICA functionalization, IFN-γ secretion rises with increasing mechanical stimulus. It must be noted that the obtained differences in the secretion of interferon-γ between the surfaces shown in Figure 3a could stem from variations in the chemical stimulus provided by MICA. To verify this, the interface between the NK cells and nanowires was closely examined by SEM (Figure 1), and by z-stack confocal microscopy (Figure S3, Supporting Information), for different nanowires. As previously[12] suggested, the cells are in contact with the upper

≈2 μm of the nanowires, regardless of nanowire length. This strongly indicates that NK cells stimulated on differently elongated nanowires were exposed to the same amount of the chemical stimulus. Given that the density of the nanowires is the same in each case, and that the surface density of MICA on the nanowires is identical, it can be concluded therefore that the cells on the nanowires were exposed to the same amount of MICA. Thus, the difference in the mechanical stimuli provided by the nanowires with different flexibilities was the reason explaining the different degrees of interferon-γ release. We cannot exclude the putative effect of differences in surface density of MICA on the difference between the activation on the nanowires and flat control. To evaluate this possibility, we compared the total number of MICA per unit area, for the cases of flat surfaces versus nanowires. To calculate the number of MICA molecules per unit area for a flat surface, we first measured the average density of Au nanoparticles on the flat control surface and found 16 NPs/μm^2, with diameters of about 50 nm (Figure S1f, Supporting Information). Assuming that nanoparticles are spherical and that only the upper hemisphere is exposed to cells, this exposed area corresponds to about 1.6×10^{-2} μm^2. Then, taking into account that functionalization process we used yields $\approx 2 \times 10^4$ MICA molecules/μm^2,[43] we deduce that the cells stimulated on the flat sample were exposed to $16*1.6 \times 10^{-2}*2 \times 10^4 = \approx 0.5 \times 10^4$ MICA molecules/μm^2. Similarly, to calculate the number of MICA molecules available for the cells on nanowires, we considered that the cells contact the upper 2 μm of nanowires, and that the average nanowire diameter and density are 50 nm and 3 nanowires/μm^2, respectively (Figure S1a–c, Supporting Information). The surface area of contact area of the nanowires is then ≈0.3 μm^2, and assuming that MICA coverage on ZnO is the same as in on Au, it can be deduced that the cells on the nanowires were exposed to $3*0.3*2 \times 10^4 = \approx 1.8 \times 10^4$ MICA molecules/μm^2. These two surface densities – on the flat control surfaces and on the top 2 μm of the nanowire forest –are of the same order of magnitude. Also, in both cases the surface density of MICA is substantially higher than the density threshold of 1000 MICA molecules/μm^2 for needed for NK cells activation.[28] Thus, NK cells on the flat control surfaces and on the nanowires are being provided a sufficient amount of MICA, resulting in the saturation of the chemical stimulus. The difference between NK cells on the flat surface and on the nanowires can be explained only by the difference in the physical stimulation on these surfaces.

The fact that the mechanical stimuli regulate the immune response of NK cells is further illustrated by NK cells stimulated on bare nanowires, which lack any chemical stimulus (Figure 3b). Here, the observed trend is the same as for MICA functionalized nanowire, i.e., the lowest amount of interferon-γ was by secreted cells stimulated on flat sapphire surfaces, while, on surfaces with nanowires, this amount gradually increased with nanowire length. On the other hand, the absolute value of interferon-γ was lower than that obtained for MICA-functionalized surfaces, both for flat surfaces and for the nanowires of each length (Figure 3c–e). This clearly indicates that MICA functionalization, while present in the same amount on the nanowires and control samples, provides a chemical stimulus which is constant, and whose contribution to the overall secretion of interferon-γ is independent of the mechanical stimulus provided by the nanowires. It is to be noted that the mechanical stimulus depends on the environmental flexibility, which is determined here by the nanowire length and activates the cells independently of the chemical stimulus. The maximal activation, as reflected by the amount of secreted interferon-γ, is produced when both the chemical and mechanical stimuli are combined. Finally, the high sensitivity of NK cells to nanowire flexibility indicates that the environmental flexibility, rather than environmental topography, is likely the dominant factor in the physical stimulation of NK cells.

To explore the effect of nanowire length on the late signaling of NK cells, we assessed the degree of nuclear translocation of the p65 subunit of NF-κB, a key transcription factor that dictates the outcome of immune response. Here, we used NF-κB as an activation marker for NK cells and quantified the p65 subunit nuclear content by quantitative immunofluorescence after incubation for 18 hours (Figure 3g). Figure 3h,i presents the average degrees of translocation per cell for the stimulating surfaces with and without MICA, respectively. It is clear that the dependence of p65 nuclear content on both nanowire length and MICA functionalization follows the same trend as previously discussed for interferon-γ. For MICA functionalized surfaces, flat sapphire induced the lowest translocation. A higher degree of translocation was obtained for cells stimulated on MICA-functionalized nanowires, and gradually increased with nanowire length. Also, similarly to interferon-γ, nuclear translocation of NF-κB produced the same trend for bare surfaces, yet its overall magnitude was systematically lower than for MICA-functionalized surfaces, although with minor differences (Figure S3, Supporting Information).

Finally, we studied the effect of the tunable mechanical stimulus provided by the nanowires on the activation of NK cells by imaging the accumulation of lysosome-associated membrane protein-1 (CD107a) on the membrane of stimulated NK cells. In activated NK cells, lytic granules that contain granzymes and perforins merge with the membrane, where they degranulate and expose CD107a. This makes CD107a a commonly used quantitative marker for the activation of NK cells. To ensure that only surface expressed CD107a is labelled, but not cytolytic CD107a, the cells were not permeabilized prior to staining. Figure 4a shows a typical confocal image of cells expressing CD107a on MICA functionalized nanowires. Here, MICA was previously labeled with TAMRA (red) to allow imaging of the nanowires, and CD107a was stained with a fluorescently tagged antibody (white). Figure 4b–g show the quantification of the average CD107a signal per cell, as a function of nanowire length and surface functionalization. For MICA functionalized surfaces (Figure 4b), the observed trend mirrors well our previous report on the increased degranulation of NK cells stimulated on MICA-functionalized nanowires.[12] However, here we gradually varied the nanowires length, and this variation provided an insight into the tunability of degranulation by changing the magnitude of the mechanical stimulus. Remarkably, the extent of degranulation does not significantly change between short and medium nanowire. On the other hand, long nanowires induced about a 2.5-fold higher degranulation than short or medium nanowires, and more than a 3-fold higher degranulation than flat surfaces. A similar dependence to the extent of mechanical stimulus produced by the nanowires was

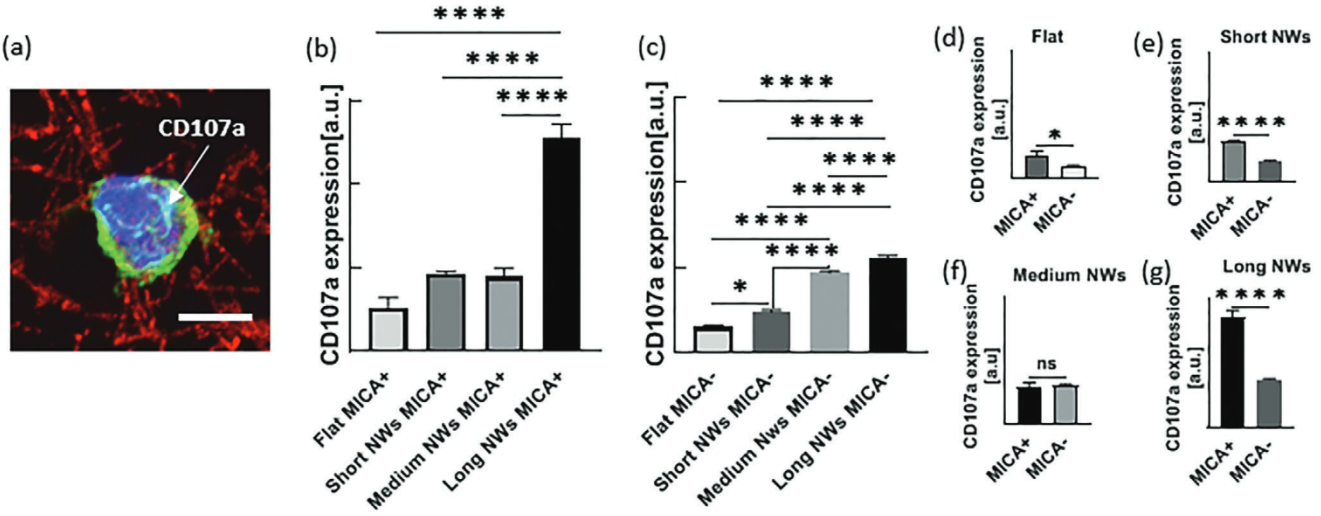

Figure 4. a) Representative image of activated NK cells on MICA-functionalized nanowires. Cells were stained with phalloidin for cytoskeleton (green), DAPI for nuclei (blue), nanowires (red) and CD107a (white). (Scale bar 5 μm). b,c) The degree of CD107a expression was quantified by measuring the fluorescence intensity of the APC-labeled anti-CD107a for surfaces with and without MICA. d–g) Effect of MICA on activation of NK cells stimulated on flat surfaces and short, medium, and long nanowires. The analysis was performed with Tukey's multiple-comparison tests using the GraphPad Prism software. *$p < 0.05$, **$p < 0.01$, ***$p < 0.001$, ****$p < 0.0001$, ns-not significant. Here (+) and (–) means surfaces with and without anti-CD3 functionalization, respectively.

obtained on non-functionalized surfaces (Figure 4c). Yet, exactly like for interferon–γ and NF-κB, the magnitude of CD107a expression on bare surfaces was systematically lower than that obtained on MICA functionalized surfaces, for all the surfaces, with the exception of medium nanowires (Figure 4d–g). This observation confirms that the mechanical and chemical stimuli are complementary, and that each stimulus can independently control the relative degree of degranulation in NK cells. Also, a high degree of degranulation would likely require both stimuli at their optimal amounts, as illustrated by the significantly higher degranulation of cells stimulated on MICA-functionalized long nanowires.

3. Discussion

This work explores, for the first time to the best of our knowledge, the sensation of NK cells to different degrees of nanomechanical stimuli provided by their environment. The first indication of this sensation was reported by us two years ago, when we showed that NK cells stimulated on MICA-functionalized nanowires produce substantially higher degranulation than their counterparts stimulated on flat rigid surfaces with similar or greater quantities of MICA. This result led to the hypothesis that NK cells are able to distinguish between independent chemical and mechanical signals produced by their environment. The results reported here not only prove this hypothesis, but also show that the mechanostimulating environment, which was modelled here by nanowires, does not only increase the activation of NK cells, but can also produce a measured amount of the mechanical stimulus that tunes the signaling and immune response of NK cells.

The response of NK cells was characterized here by three independent figures of merit – production of interferon-γ, nuclear translocation of NF-κB, and expression of CD107a. It was not surprising that all three showed an almost identical dependence on the nanowire geometry and surface functionalization with MICA. Indeed, NF-κB nuclear translocation is involved in perforin expresson,[42] which, in turn, is closely associated with CD107a expression since both are outcomes of NK cells degranulation.[44] Similarly, nuclear translocation of NF-κB was shown to be highly correlated with the degree of cytotoxic activity of NK cell function, which results in the release of interferon-γ.[45] Thus, the coherence in all three responses characterized here is a clear indication that they are similarly regulated by the mechanical stimulus provided by the NK cell environment, at least on a qualitative level. Further studies should be aimed at gaining a deeper understanding of the fundamental mechanism of NK cells mechanosensation. Recently, we showed that the clustering a costimulatory receptor DAP10 in NK cells is highly affected by the elastic modulus of the stimulating surfaces.[46] Clustering of DAP10 is closely associated with that of NKG2D,[47,48] which, in turn, requires remodeling of actin[21]. It is possible, therefore, that the mechanical compliance of the nanowires indirectly affects the clustering of NKG2D that is necessary for the activation of NK cells via actin reorganization, and thereby determines the immune response of NK cells to the nanowire geometry. The mechanisms whereby NK cells mechanically sense their environment should be further explored, and they are the subject of our ongoing research.

Besides the insight into NK cell mechanosensing, our work provides an intriguing perspective on a new type of biological application of nanomaterials. During the last decade and a half, there has been an emerging interest in biological applications of nanowires, whose small dimensions make them attractive for sensing and manipulating miniature components in living cells and tissues.[49,50] Such applications include but are not

limited to the delivery of biomolecules into the cytosol,[51–53] studying cell morphology,[54] mechanostimulation and mechanosensing,[55–58] and intracellular detection of electrical signals.[59,60] In our paper, we describe how nanowires can be applied to provide a deterministic and precise mechanical stimulation for NK cells. An advantage of nanowires for this application is due to their high mechanical compliance, which can be tuned in a robust and facile manner through nanowire dimensions and density. For instance, doubling the nanowire length changes its shear bending modulus by almost an order of magnitude. Lengths of nanowires produced by CVD can range from a few hundred nanometers to a few hundreds of micrometers, and their diameter and density can be precisely controlled by nanolithographic patterning of catalyst. Together, all these parameters can be tuned to engineer a microenvironment for the NK cell mechanostimulation with a broad range of stiffnesses – from hundreds of Pa to a few hundred kPa. This range mimics the natural mechanical environment of lymphocytes, which is very diverse, and includes relatively soft myeloid, monocyte, and dendritic cells whose stiffness ranges in hundreds to thousands of Pa,[39] as well as harder extracellular matrix and tumor cells and tissues whose stiffness can reach 100 kPa.[61,62] Besides lymphocytes such as NK cells, nanowire-based mechanostimulation platforms can be generalized and applied to numerous mechanobiology studies of other cells, such as cancer cells.

4. Conclusion

This study fills the last missing element in the puzzle of lymphocyte mechanosensing. Among the three types of lymphocytes, T cells are the ones whose mechanosensing has been most studied. This includes an early study of Judokusumo et al. that showed that Naïve CD4+ T cell increase the secretion of IL-2 with an increase in the elasticity of the stimulating surface for a range of 10–200 kPa, and that this elasticity modulates the downstream signaling of the T cell receptor.[8] Later, the effect of surface elasticity on the activation of CD4+ T cells was studied for a lower range of elasticity down to 0.5 kPa, showing, nevertheless, the same trend in activation versus elasticity.[41] Finally, mechanosensing was also demonstrated for CD8+ T cells.[40,63] Similarly, the mechanosensing of B cells was demonstrated as well, on stimulating surfaces of varying elasticities.[9,10] In contrast, how NK cells mechanically sense their environment has remained obscure, and this work provides an illuminating insight on this important yet still largely unstudied aspect of NK cell function, and can be used to conclude that mechanosensing is a generic feature of all the three types of lymphocytes, although it might involve different mechanisms in each case.[7]

Understanding how the cytotoxic activity of NK cells is regulated by physical stimuli is not only fundamentally important but also has an applied significance. NK cell based immunotherapy is a promising and extensively explored approach for cancer treatment.[64–66] Yet, the ex vivo activation of NK cells, which is a critical step in the immunotherapy process,[67] remains a challenge. Common approaches include activation by cytokine supply, which, however, cannot alone sustain NK cell proliferation,[68] feeder cells, which, on the downside, may result in unpredictable risks,[69] or artificial antigen presenting cells, whose production is relatively complex.[70] Alternatively, micro-/nano-scale structures rationally designed to combine activating biochemical and mechanical/nanotopographical stimuli were recently shown for effective ex vivo activation of T cells.[71–74] This approach can also be naturally applied to NK cells, thus making antigen-functionalized nanowires a promising candidate as a functional nanomaterial that can be used for NK cell chemo-mechano-activation in future immunotherapies.

Supporting Information

Supporting Information is available from the Wiley Online Library or from the author.

Acknowledgements

This work was funded by the Multidisciplinary Research Grant – The Faculty of Health Science in Ben-Gurion University of the Negev. Israel Science Fousndation, Individual Grant # 1401/15 and Israel Science Foundations: F.I.R.S.T. Individual Grant # 2058/18. V. Bhingardive thanks the Negev-Tsin scholarship for its support.

Conflict of Interest

The authors declare no conflict of interest.

Data Availability Statement

Research data are not shared.

Keywords

activation, biofunctionalization, mechanosensing, nanowires, NK cells

Received: March 30, 2021
Published online:

[1] R. B. Herberman, M. E. Nunn, D. H. Lavrin, *Int. J. Cancer* **1975**, *16*, 216.
[2] R. Kiessling, E. Klein, H. Pross, H. Wigzell, *Eur. J. Immunol.* **1975**, *5*, 117.
[3] M. J. Smyth, Y. Hayakawa, K. Takeda, H. Yagita, *Nat. Rev. Cancer* **2002**, *2*, 850.
[4] E. M. Mace, J. S. Orange, *Front. Immunol.* **2013**, *3*, 421.
[5] J. S. Orange, *Nat Rev. Immunol.* **2008**, *8*, 713.
[6] D. M. Davis, I. Chiu, M. Fassett, G. B. Cohen, O. Mandelboim, J. L. Strominger, *Proc. Natl. Acad. Sci. USA* **1999**, *96*, 15062.
[7] M. Huse, *Nat. Rev. Immunol.* **2017**, *17*, 679.
[8] E. Judokusumo, E. Tabdanov, S. Kumari, M. L. Dustin, L. C. Kam, *Biophys. J.* **2012**, *102*, L5.
[9] Y. Zeng, J. Yi, Z. Wan, K. Liu, P. Song, A. Chau, F. Wang, Z. Chang, W. Han, W. Zheng, Y. H. Chen, C. Xiong, W. Liu, *Eur. J. Immunol.* **2015**, *45*, 1621.

[10] Z. Wan, S. Zhang, Y. Fan, K. Liu, F. Du, A. M. Davey, H. Zhang, W. Han, C. Xiong, W. Liu, *J. Immunol.* **2013**, *190*, 4661.
[11] O. Matalon, A. Ben-Shmuel, J. Kivelevitz, B. Sabag, S. Fried, N. Joseph, E. Noy, G. Biber, M. Barda-Saad, *EMBO J.* **2018**, *37*, 96264.
[12] G. L. Saux, N. Bar-Hanin, A. Edri, U. Hadad, A. Porgador, M. Schvartzman, *Adv. Mater.* **2019**, *31*, 1805954.
[13] P. Verdijk, P. A. van Veelen, A. H. de Ru, P. J. Hensbergen, K. Mizuno, H. K. Koerten, F. Koning, C. P. Tensen, A. M. Mommaas, *Eur. J. Immunol.* **2004**, *34*, 156.
[14] M. Draghi, A. Pashine, B. Sanjanwala, K. Gendzekhadze, C. Cantoni, D. Cosman, A. Moretta, N. M. Valiante, P. Parham, *J. Immunol.* **2007**, *178*, 2688.
[15] T. Ebihara, H. Masuda, T. Akazawa, M. Shingai, H. Kikuta, T. Ariga, M. Matsumoto, T. Seya, *Int. Immunol.* **2007**, *19*, 1145.
[16] M. Jinushi, T. Takehara, T. Kanto, T. Tatsumi, V. Groh, T. Spies, T. Miyagi, T. Suzuki, Y. Sasaki, N. Hayashi, *J. Immunol.* **2003**, *170*, 1249.
[17] A. P. Trembath, M. A. Markiewicz, *Front. Immunol.* **2018**, *9*, 231.
[18] D. Blumenthal, V. Chandra, L. Avery, J. K. Burkhardt, *Elife* **2020**, *9*, 1.
[19] M. Arnold, E. A. Cavalcanti-Adam, R. Glass, J. Blümmel, W. Eck, M. Kantlehner, H. Kessler, J. P. Spatz, *ChemPhysChem* **2004**, *5*, 383.
[20] M. Schvartzman, M. Palma, J. Sable, J. Abramson, X. Hu, M. P. Sheetz, S. J. Wind, *Nano Lett.* **2011**, *11*, 1306.
[21] R. Changede, H. Cai, S. J. Wind, M. P. Sheetz, *Nat. Mater.* **2019**, *18*, 1366.
[22] R. Oria, T. Wiegand, J. Escribano, A. Elosegui-Artola, J. J. Uriarte, C. Moreno-Pulido, I. Platzman, P. Delcanale, L. Albertazzi, D. Navajas, X. Trepat, J. M. García-Aznar, E. A. Cavalcanti-Adam, P. Roca-Cusachs, *Nature* **2017**, *552*, 219.
[23] M. J. Dalby, N. Gadegaard, R. Tare, A. Andar, M. O. Riehle, P. Herzyk, C. D. W. Wilkinson, R. O. C. Oreffo, *Nat. Mater.* **2007**, *6*, 997.
[24] J. Matic, J. Deeg, A. Scheffold, I. Goldstein, J. P. Spatz, *Nano Lett.* **2013**, *13*, 5090.
[25] J. Deeg, M. Axmann, J. Matic, A. Liapis, D. Depoil, J. Afrose, S. Curado, M. L. Dustin, J. P. Spatz, *Nano Lett.* **2013**, *13*, 5619.
[26] D. Delcassian, D. Depoil, D. Rudnicka, M. Liu, D. M. Davis, M. L. Dustin, I. E. Dunlop, *Nano Lett.* **2013**, *13*, 5608.
[27] H. Cai, J. Muller, D. Depoil, V. Mayya, M. P. Sheetz, M. L. Dustin, S. J. Wind, *Nat. Nanotechnol.* **2018**, *13*, 610.
[28] Y. Keydar, G. L.e Saux, A. Pandey, E. Avishay, N. Bar-Hanin, T. Esti, V. Bhingardive, U. Hadad, A. Porgador, M. Schvartzman, *Nanoscale* **2018**, *10*, 14651.
[29] F. Pi, P. Dillard, R. Alameddine, E. Benard, A. Wahl, I. Ozerov, A. Charrier, L. Limozin, K. Sengupta, *Nano Lett.* **2015**, *15*, 5178.
[30] N. G. Caculitan, H. Kai, E. Y. Liu, N. Fay, Y. Yu, T. Lohmüller, G. P. O'Donoghue, J. T. Groves, *Nano Lett.* **2014**, *14*, 2293.
[31] W. Il Park, G. Zheng, X. Jiang, B. Tian, C. M. Lieber, *Nano Lett.* **2008**, *8*, 3004.
[32] P. Xie, Y. Hu, Y. Fang, J. Huang, C. M. Lieber, *Proc. Natl. Acad. Sci. USA* **2009**, *106*, 15254.
[33] Y. Cui, L. J. Lauhon, M. S. Gudiksen, J. Wang, C. M. Lieber, *Appl. Phys. Lett.* **2001**, *78*, 2214.
[34] L. D. Landau, E. M. Lifshiĭs, A. M. Kosevich, L. P. Pitaevskiĭ, *Theory of Elasticity*, Butterworth-Heinemann, Oxford **1986**.
[35] Y. Huang, X. Bai, Y. Zhang, *J. Phys. Condens. Matter* **2006**, *18*, L179.
[36] X. D. Bai, P. X. Gao, Z. L. Wang, E. G. Wang, *Appl. Phys. Lett.* **2003**, *82*, 4806.
[37] H. Ni, X. Li, *Nanotechnology* **2006**, *17*, 3591.
[38] J. Song, X. Wang, E. Riedo, Z. L. Wang, *Nano Lett.* **2005**, *5*, 1954.
[39] N. Bufi, M. Saitakis, S. Dogniaux, O. Buschinger, A. Bohineust, A. Richert, M. Maurin, C. Hivroz, A. Asnacios, *Biophys. J.* **2015**, *108*, 2181.
[40] R. S. O'Connor, X. Hao, K. Shen, K. Bashour, T. Akimova, W. W. Hancock, L. C. Kam, M. C. Milone, *J. Immunol.* **2012**, *189*, 1330.
[41] M. Saitakis, S. Dogniaux, C. Goudot, N. Bufi, S. Asnacios, M. Maurin, C. Randriamampita, A. Asnacios, C. Hivroz, *Elife* **2017**, *6*, e23190.
[42] J. Zhou, J. Zhang, M. G. Lichtenheld, G. G. Meadows, *J. Immunol.* **2002**, *169*, 1319.
[43] G. L.e Saux, A. Edri, Y. Keydar, U. Hadad, A. Porgador, M. Schvartzman, *ACS Appl. Mater. Interfaces* **2018**, *10*, 11486.
[44] K. Krzewski, A. Gil-Krzewska, V. Nguyen, G. Peruzzi, J. E. Coligan, *Blood* **2013**, *121*, 4672.
[45] H. J. Kwon, G. E. Choi, S. Ryu, S. J. Kwon, S. C. Kim, C. Booth, K. E. Nichols, H. S. Kim, *Nat. Commun.* **2016**, *7*, 1.
[46] L. Mordechay, G. L.e Saux, A. Edri, U. Hadad, A. Porgador, M. Schvartzman, *ACS Biomater. Sci. Eng.* **2021**, *7*, 122.
[47] L. Quatrini, R. Molfetta, B. Zitti, G. Peruzzi, C. Fionda, C. Capuano, R. Galandrini, M. Cippitelli, A. Santoni, R. Paolini, *Sci. Signal.* **2015**,.
[48] Š. Bálint, F. B. Lopes, D. M. Davis, *Sci. Signal.* **2018**, *11*, eaal3606.
[49] C. N. Prinz, *J. Phys. Condens. Matter* **2015**, *27*, 233103.
[50] T. Berthing, S. Bonde, C. B. Sørensen, P. Utko, J. Nygård, K. L. Martinez, *Small* **2011**, *7*, 640.
[51] A. K. Shalek, J. T. Robinson, E. S. Karp, J. S. Lee, D. R. Ahn, M. H. Yoon, A. Sutton, M. Jorgolli, R. S. Gertner, T. S. Gujral, G. MacBeath, E. G. Yang, H. Park, *Proc. Natl. Acad. Sci. USA* **2010**, *107*, 1870.
[52] J. T. Robinson, M. Jorgolli, A. K. Shalek, M. H. Yoon, R. S. Gertner, H. Park, *Nat. Nanotechnol.* **2012**, *7*, 180.
[53] A. K. Shalek, J. T. Gaublomme, L. Wang, N. Yosef, N. Chevrier, M. S. Andersen, J. T. Robinson, N. Pochet, D. Neuberg, R. S. Gertner, I. Amit, J. R. Brown, N. Hacohen, A. Regev, C. J. Wu, H. Park, *Nano Lett.* **2012**, *12*, 6498.
[54] T. Berthing, S. Bonde, K. R. Rostgaard, M. H. Madsen, C. B. Sorensen, J. Nygård, K. L. Martinez, *Nanotechnology* **2012**, *23*, 415102.
[55] C. S. Hansel, S. W. Crowder, S. Cooper, S. Gopal, M. Joaio Pardelha Da Cruz, L. De Oliveira Martins, D. Keller, S. Rothery, M. Becce, A. E. G. Cass, C. Bakal, C. Chiappini, M. M. Stevens, *ACS Nano* **2019**, *13*, 2913.
[56] Z. Li, J. Song, G. Mantini, M. Y. Lu, H. Fang, C. Falconi, L. J. Chen, Z. L. Wang, *Nano Lett.* **2009**, *9*, 3575.
[57] W. Hallstrom, M. Lexholm, D. B. Suyatin, G. Hammarin, D. Hessman, L. Samuelson, L. Montelius, M. Kanje, C. N. Prinz, *Nano Lett.* **2010**, *10*, 782.
[58] P. K. Sahoo, R. Janissen, M. P. Monteiro, A. Cavalli, D. M. Murillo, M. V. Merfa, C. L. Cesar, H. F. Carvalho, A. A. De Souza, E. P. A. M. Bakkers, *Nano Lett.* **2016**, *16*, 4656.
[59] T. Cohen-Karni, B. P. Timko, L. E. Weiss, C. M. Lieber, *Proc. Natl. Acad. Sci. USA* **2009**, *106*, 7309.
[60] B. P. Timko, T. Cohen-Karni, G. Yu, Q. Qing, B. Tian, C. M. Lieber, *Nano Lett.* **2009**, *9*, 914.
[61] S. Kawano, M. Kojima, Y. Higuchi, M. Sugimoto, K. Ikeda, N. Sakuyama, S. Takahashi, R. Hayashi, A. Ochiai, N. Saito, *Cancer Sci.* **2015**, *106*, 1232.
[62] M. J. Paszek, N. Zahir, K. R. Johnson, J. N. Lakins, G. I. Rozenberg, A. Gefen, C. A. Reinhart-King, S. S. Margulies, M. Dembo, D. Boettiger, D. A. Hammer, V. M. Weaver, *Cancer Cell* **2005**, *8*, 241.
[63] R. Basu, B. M. Whitlock, J. Husson, A. L.e Floc'h, W. Jin, A. Oyler-Yaniv, F. Dotiwala, G. Giannone, C. Hivroz, N. Biais, J. Lieberman, L. C. Kam, M. Huse, *Cell* **2016**, *165*, 100.
[64] L. Baggio, Á. M. Laureano, L. M. da R. Silla, D. A. Lee, *Clin. Immunol.* **2017**, *177*, 3.
[65] C. Guillerey, N. D. Huntington, M. J. Smyth, *Targeting natural killer cells in cancer immunotherapy*, Vol. *17*, Nature Publishing Group, **2016**, pp. 1025–1036.

[66] M. Cheng, Y. Chen, W. Xiao, R. Sun, Z. Tian, *NK cell-based immunotherapy for malignant diseases*, Vol. *10*, Nature Publishing Group, **2013**, pp. 230–252.
[67] M. Granzin, J. Wagner, U. Köhl, A. Cerwenka, V. Huppert, E. Ullrich, *Shaping of natural killer cell antitumor activity by ex vivo cultivation 8*, Frontiers Media S.A., **2017**, p. 1.
[68] J. Shi, G. Tricot, S. Szmania, N. Rosen, T. K. Garg, P. A. Malaviarachchi, A. Moreno, B. DuPont, K. C. Hsu, L. A. Baxter-Lowe, M. Cottler-Fox, J. D. Shaughnessy, B. Barlogie, F. Van Rhee, *Br. J. Haematol.* **2008**, *143*, 641.
[69] H. Fujisaki, H. Kakuda, N. Shimasaki, C. Imai, J. Ma, T. Lockey, P. Eldridge, W. H. Leung, D. Campana, *Cancer Res.* **2009**, *69*, 4010.
[70] S. S. Somanchi, V. V. Senyukov, C. J. Denman, D. A. Lee, *J. Vis. Exp.* **2010**, 2540.
[71] L. H. Lambert, G. K. E. Goebrecht, S. E. De Leo, R. S. O'Connor, S. Nunez-Cruz, T. De Li, J. Yuan, M. C. Milone, L. C. Kam, *Nano Lett.* **2017**, *17*, 821.
[72] A. P. Dang, S. De Leo, D. R. Bogdanowicz, D. J. Yuan, S. M. Fernandes, J. R. Brown, H. H. Lu, L. C. Kam, *Adv. Biosyst.* **2018**, *2*, 1700167.
[73] T. R. Fadel, F. A. Sharp, N. Vudattu, R. Ragheb, J. Garyu, D. Kim, E. Hong, N. Li, G. L. Haller, L. D. Pfefferle, S. Justesen, K. C. Harold, T. M. Fahmy, *Nat. Nanotechnol.* **2014**, *9*, 639.
[74] A. S. Cheung, D. K. Y. Zhang, S. T. Koshy, D. J. Mooney, *Nat. Biotechnol.* **2018**, *36*, 160.